ETRI Journal, Volume 39, Number 6, December 2017
http://onlinelibrary.wiley.com/journal/10.4218/(ISSN)2233-7326

Full-Duplex Operations in Wireless Powered Communication Networks

Hyungsik Ju, Yuro Lee, and Tae-Joong Kim

In this paper, a wireless powered communication network (WPCN) consisting of a hybrid access point (H-AP) and multiple user equipment (UE), all of which operate in full-duplex (FD), is described. We first propose a transceiver structure that enables FD operation of each UE to simultaneously receive energy in the downlink (DL) and transmit information in the uplink (UL). We then provide an energy usage model in the proposed UE transceiver that accounts for the energy leakage from the transmit chain to the receive chain. It is shown that the throughput of an FD WPCN using the proposed FD UE (FD-WPCN-FD) can be maximized by optimal allocation of the UL transmission time to the UE by solving a convex optimization problem. Simulation results reveal that the use of the proposed FD UE efficiently improves the throughput of a WPCN with a practical self-interference cancellation capability at the H-AP. Compared to the WPCN with FD H-AP and half-duplex (HD) UE, FD-WPCN-FD achieved an 18% throughput gain. In addition, the throughput of FD-WPCN-FD was shown to be 25% greater than that of WPCN in which an H-AP and UE operated in HD.

Keywords: Energy harvesting (EH), Full duplex, Simultaneous transmission and reception, Wireless-powered communication network (WPCN), Wireless energy transfer.

I. Introduction

A growing interest in harvesting energy from far-field radio-frequency (RF) signal transmissions has emerged as a novel means of powering mobile devices. In particular, the design of a wireless-powered communication network (WPCN) has been studied as a significant application of RF energy harvesting, whereby remote user equipment (UE) utilizes the energy harvested from a wireless RF power transfer for wireless communications. A typical WPCN model was proposed in [1]. In this model, a wireless energy transfer (WET) in the downlink (DL) and wireless information transmission (WIT) in the uplink (UL) are both coordinated by a hybrid access point (H-AP). In a WPCN in which the H-AP and UE all operate in half-duplex (HD) mode—an HD-WPCN—a fundamental trade-off exists in allocating resources to the DL for a WET and the UL for a WIT [1]. This is because allocating more resources to the DL for a WET increases the transmit power of the UEs in the UL owing to the increase in the amount of harvested energy, while also decreasing the resources allocated to the UL for a WIT.

Meanwhile, full-duplex (FD) based wireless systems—in which the wireless nodes simultaneously transmit and receive RF signals in the same frequency band—have received considerable attention. FD operation is expected to potentially double the spectral efficiency in wireless communications by cancelling the self-interference (SI) that occurs through the leakage of a transmitted signal received by the transmitting node itself. In particular, the feasibility of FD communication has been verified through a proof-of-concept design, which shows that the power of the residual SI after self-interference cancellation (SIC) is applied is reduced to a level sufficiently close to that of background noise [2], [3].

Manuscript received Mar. 23, 2017; revised July 25, 2017; accepted July 28, 2017.

Hyungsik Ju (corresponding author, jugun@etri.re.kr), Yuro Lee (yurolee@etri.re.kr), and Tae-Joong Kim (aisma@etri.re.kr) are with 5G Giga Service Research Laboratory, ETRI, Daejeon, Rep. of Korea.

https://doi.org/10.4218/etrij.17.0117.0217 pISSN: 1225-6463, eISSN: 2233-7326

The simultaneous transmission and reception of an FD operation can also improve the WPCN throughput. In [4], a WPCN model was proposed in which an H-AP with an FD operation coordinates both a wireless energy transfer to and a wireless information transmission from a set of UEs operating in HD mode. This is denoted as FD-WPCN with HD UE (FD-WPCN-HD). It was shown in [4] that the FD operation of an H-AP in an FD-WPCN-HD can increase the throughput of a WPCN when the SI is sufficiently cancelled out. In [5], the authors studied resource allocation in an FD-WPCN-HD using an energy causality constraint, which is a constraint in which the signal transmission of a UE at a given time can utilize only the energy harvested during a previous time. An FD-WPCN-HD with orthogonal frequency-division multiplexing (OFDM) modulation was further studied in [6]. Finally, in [7], a wireless powered relay network was investigated in which an FD relay that utilizes SI as an energy source relays information of an HD source to an HD destination.

In the present study, we examined another type of WPCN, in which not only the H-AP, but also the UE, operate in FD mode, denoted by FD-WPCN with FD UE (FD-WPCN-FD). Owing to the FD capability, UE can receive the signal sent by the H-AP to carry energy while transmitting the respective UL information. We first propose a transceiver structure for UE that enables simultaneous energy reception in the DL and information transmission in the UL. By extending our previous work [8], we characterize the energy usage in the proposed UE transceiver, accounting for an energy leakage from the transmit chain to the receive chain. Additionally, we show that the UE can harvest energy from the leakage of its own UL transmissions (in other words, SI) as well as the received signal sent by the H-AP in the DL. Finally, based on a time-division-multiple-access (TDMA) protocol for WIT in the UL, the optimal time allocation to maximize the weighted sum-throughput in the network, subject to a given total time constraint, is described.

The remainder of this paper is organized as follows. Section II presents the FD-WPCN-FD system model and the proposed UE structure. In Section III, we examine the FD-WPCN-FD throughput and resource allocation to maximize the throughput. Section IV provides simulation results on the FD-WPCN-FD throughput. Finally, Section V concludes this paper.

II. System Model

Figure 1 shows the FD-WPCN-FD model considered in this paper. This network consists of one H-AP and K UE (denoted by U_i, $i = 1, \dots, K$), all of which are equipped with a single-antenna FD transceiver to simultaneously transmit and receive signals over the same frequency band.

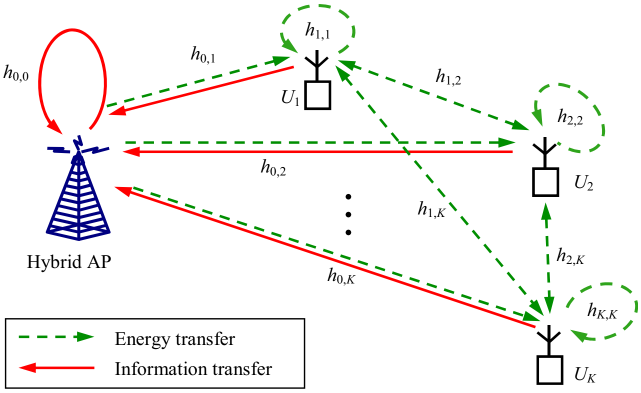

Fig. 1. WPCN model with an FD H-AP and FD UE.

The H-AP transfers energy to the UE in the DL by broadcasting a signal dedicated to carrying energy. At the same time, the H-AP receives signals transmitted by the UEs in the UL, which contains information for decoding. The FD operation of the H-AP enables the simultaneous transmission/reception of energy/information signals in the DL/UL, respectively. For decoding information received in the UL, an SI canceller is deployed at the FD transceiver of the H-AP to eliminate SI (in other words, the leakage of a DL energy signal transmission received by itself), which interferes with the reception of the UL information signals.

On the other hand, UE harvests energy from the received signals and charges its respective batteries. A portion of the charged energy is used to transmit information in the UL. On account of the FD operation, UE can simultaneously transmit/receive information/energy signals in the UL/DL, respectively. This is enabled by the transceiver shown in Fig. 2. Note that the energy signal broadcasted by the H-AP in the DL carries no information for decoding; it only carries energy. Therefore, neither an information decoder nor an SI canceller is deployed at the receiving end of a UE

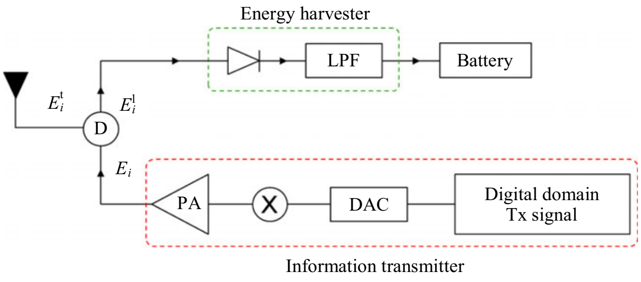

Fig. 2. Transceiver structure for FD UE.

transceiver. Instead, an energy harvester (for example, a rectifier) is installed at the receiving end to harvest energy from the received signals.

Note that, in this transceiver, a portion of the power amplifier (PA) output energy at the transmitting end leaks into the receiving end as SI on account of the circulator loss (duplexer loss), whereas the remaining portion of the PA output energy is used to transmit information to the H-AP. At the ith user U_i, as shown in Fig. 2, E_i, E_i^{l}, and E_i^{t} represent the PA output energy at the transmitting end, energy leaking into the receiving end as SI, and energy used to transmit information, respectively, where $E_i = E_i^{\mathrm{l}} + E_i^{\mathrm{t}}$. For convenience, E_i^{l} and E_i^{t} are given, respectively, by

$$E_i^{\mathrm{l}} = \varphi_i E_i \quad \text{and} \quad E_i^{\mathrm{t}} = (1-\varphi_i)E_i,\ 0 \le \varphi_i \le 1,^{1)} \tag{1}$$

where φ_i represents the circulator loss at the transceiver of U_i. At the proposed transceiver, a trade-off is yielded by the value of φ_i because, as φ_i increases, the energy harvested from SI increases, whereas the energy used for WIT decreases.

In the network shown in Fig. 1, a signal transmission from U_i to U_j, $\forall i, j \in \{0, \ldots, K\}$, is assumed to pass through a complex channel, $h_{i,j}$, with the channel power gain given by $H_{i,j} = |h_{i,j}|^2$ (U_0 represents the H-AP later herein). In particular, when $i = j$, $h_{i,i}$ represents the SI channel at U_i through which the leakage signal of U_i is received by itself. It is assumed that the channels remain constant during a block transmission time denoted by T (in other words, following quasi-static flat-fading), and $h_{i,j} = h_{j,i}$ with the channel reciprocity. The H-AP is assumed to have perfect knowledge of $h_{0,i}$, $\forall i \in \{0, \ldots, K\}$. Furthermore, φ_i, $\forall i \in \{0, \ldots, K\}$, is also assumed to be known by the H-AP.

Figure 3 shows a transmission protocol for FD-WPCN-FD. During the whole block duration, T, the H-AP transmits an energy signal with constant power P_0 in the DL, which is received by all UE. While broadcasting energy by the H-AP, the UE transmits its own independent information to the H-AP in the UL orthogonally over time through a TDMA. The transmission block therefore consists of K slots, each of which is allocated to U_i for the UL information transmission. The duration of the ith slot is given by $\tau_i T$, $i = 1, \ldots, K$, where

$$\sum_{i=1}^{K} \tau_i \le 1, \quad 0 \le \tau_i \le 1. \tag{2}$$

During the ith slot, the H-AP and user U_i transmit a DL signal to carry energy and a UL signal to carry information, respectively. Therefore, the received signals at the H-AP and U_i, $i \ne 0$, during the ith slot can be expressed, respectively, as

$$y_{i,0} = \sqrt{P_i} h_{0,i} x_i + \sqrt{P_0} h_{0,0} x_0 + n_0, \tag{3}$$

$$y_{i,i} = \sqrt{P_0} h_{0,i} x_0 + \sqrt{P_i} h_{i,i} x_i + n_i, \tag{4}$$

with x_k, $\forall k = 0, \ldots, K$, denoting the transmitted signal of U_k with $\boldsymbol{E}[|x_k|^2] = 1$, where $\boldsymbol{E}[\mu]$ represents the expectation of a random variable, μ. Furthermore, P_k represents the transmit power of U_k, $\forall k = 0, \ldots, K$. Finally, n_k denotes the receiver noise at U_k, $\forall k = 0, \ldots, K$. It is assumed that $n_k \sim CN(0, \sigma_i^2)$, with $CN(v, \sigma^2)$ representing a circularly symmetric complex Gaussian random variable with mean v and variance σ^2. It is worth noting that the H-AP must decode x_i in (3), whereas U_i does not decode information in the DL. At its respective receiving ends, therefore, the H-AP must cancel the leakage of its own transmission acting as SI (the second term in (3)), whereas it is not necessary for U_i to cancel the leakage of its own transmission (the second term in (4)).

In addition, the inactive UE during the ith slot, in other words, U_j with $j \ne 0$ and $j \ne i$, also receives signals from the transmissions of the H-AP and U_i. At an inactive UE U_j, $j \ne i$, therefore, the received signal during the ith slot is given by

$$y_{i,j} = \sqrt{P_0} h_{0,j} x_0 + \sqrt{P_i} h_{i,j} x_i + n_j. \tag{5}$$

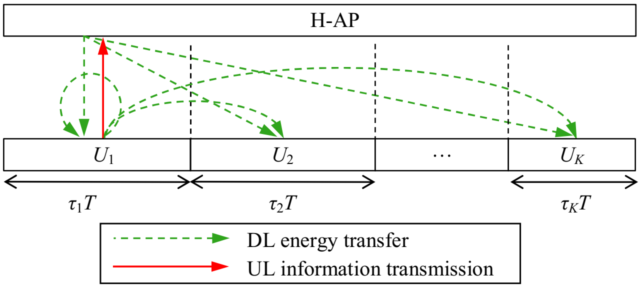

Fig. 3. Transmission protocol for FD-WPCN-FD.

III. Throughput of FD-WPCN with FD UE

In this section, the achievable throughput of the FD-WPCN-FD presented in Section II is described. In particular, we aim to maximize the weighted sum throughput of information transmissions in the UL.

[1)] When the transmitting and receiving antennas of a UE are separated, φ_i models the near-field energy absorption by the receiving antenna.

https://doi.org/10.4218/etrij.17.0117.0217

1. Achievable UL Throughput of Each UE

According to the channel knowledge available at the H-AP, the throughput of the proposed FD-WPCN-FD can be obtained with two approaches. The first assumes a full knowledge of channels by an aid of a "genie," whereas the other assumes partial channel knowledge in a more practical sense.

1) Ideal throughput achievable by a genie-aided approach. A UE, U_i, can harvest energy from the received DL signals transmitted by the H-AP (in other words, the first term in (4)) during the whole block duration. In addition, U_i can also harvest energy from the leakage of its own transmission during the *i*th slot allocated to it for a UL information transmission (in other words, the second term in (4)). Furthermore, UL transmissions of other UEs received by U_i can also be used for energy harvesting (EH) of U_i. In particular, the energy harvested from the transmissions of other UE can be considered to optimize throughput when the H-AP is assumed to have a global knowledge of channels. In other words, $H_{i,j}$, $i, j \in \{0, \ldots, K\}$, $i \neq j$, $i \neq 0, j \neq 0$, as well as $h_{0,i}$ and φ_i, $\forall i \in \{0, \ldots, K\}$. In this case, the harvested energy of U_i during a block duration T, denoted by E_i^{h}, can be obtained from (4) and (5) as

$$E_i^{\mathrm{h}} = \zeta_i \left(P_0 H_{0,i} + \tau_i P_i H_{i,i} + \sum_{j=1,\, j \neq i}^{K} \tau_j P_j H_{j,i} \right) T, \tag{6}$$

where $0 \le \zeta_i \le 1$, $i = 1, \ldots, K$ denotes the energy harvesting efficiency at U_i. The energy harvesting efficiency accounts for RF direct current (DC) conversion efficiency of a rectifier because it represents the ratio of the energy of the received signal (RF) converted into the energy harvested and stored (DC). In (6), assuming that the amount of energy harvested from the receiver noise is small enough to be neglected [1], such energy is not considered.

In the FD UE transceiver shown in Fig. 2, based on the law of energy conservation, the energy harvested from the leakage of its own transmission—$\tau_i P_i H_{i,i} T$ in (6)—is equivalent to the amount of energy leaking from the transmitting end into the receiving end. From (1), we therefore have

$$\tau_i P_i H_{i,i} T = E_i^{\mathrm{l}} = \varphi_i E_i. \tag{7}$$

In each transmission block, a portion of the harvested energy is used to generate the PA output signal at the transmitting end of the transceiver, as shown in Fig. 2. The energy of the PA output signal at U_i is then given by

$$E_i = \eta_i E_i^{\mathrm{h}}, \tag{8}$$

with $0 \le \eta_i \le 1$, $i = 1, \ldots, K$ denoting the portion of the harvested energy used to generate a PA output signal at U_i under a steady state.[2] Note that E_i^{t} in (1) can be represented as

$$E_i^{\mathrm{t}} = \tau_i P_i T = (1 - \varphi_i) E_i. \tag{9}$$

From (6) through (9), we then have

$$\begin{aligned} E_i^{\mathrm{h}} &= \zeta_i \left(P_0 H_{0,i} + \frac{\varphi_i \tau_i P_i}{1 - \varphi_i} + \sum_{j=1, j \neq i}^{K} \tau_j P_j H_{j,i} \right) T \\ &= \frac{\tau_i P_i T}{\eta_i (1 - \varphi_i)}, \end{aligned} \tag{10}$$

from which we have

$$\left(\frac{1 - \theta_i \varphi_i}{1 - \varphi_i} \right) \tau_i P_i - \theta_i \sum_{j=1,\, j \neq i}^{K} \tau_j P_j H_{j,i} = \theta_i P_0 H_{0,i}, \tag{11}$$

where $\theta_i = \eta_i \zeta_i$. It then follows that

$$\mathbf{A} \boldsymbol{\Omega} \mathbf{P} = P_0 \mathbf{b}, \tag{12}$$

where $\mathbf{P} = [P_1, P_2, \ldots, P_K]^T$ and $\boldsymbol{\Omega} = \mathrm{diag}\{[\tau_1, \tau_2, \ldots, \tau_K]^T\}$, with $\mathrm{diag}\{\mathbf{v}\}$ denoting a diagonal matrix, of which the diagonal entries consist of vector $\mathbf{v}$. Furthermore, $\mathbf{A}$ is a matrix with

$$A_{i,j} = \begin{cases} (1 - \theta_i \varphi_i)/(1 - \varphi_i) & , \text{ if } j = i, \\ -\theta_i H_{i,j} & , \text{ otherwise}, \end{cases} \tag{13}$$

where $A_{i,j}$ denotes the element of matrix $\mathbf{A}$ on the *i*th row and *j*th column. Finally, $\mathbf{b}$ is a vector given by

$$\mathbf{b} = \left[\theta_1 H_{0,1} \; \theta_2 H_{0,2} \; \cdots \; \theta_K H_{0,K} \right]^T. \tag{14}$$

From (12) through (14), P_i is then given by

$$P_i = \rho_i \frac{P_0}{\tau_i}, \; i = 1, \ldots, K, \tag{15}$$

where ρ_i, $i = 1, \ldots, K$, is given by

$$[\rho_1, \; \rho_2, \; \ldots, \; \rho_K]^T = \mathbf{A}^{-1} \mathbf{b}. \tag{16}$$

Note that at the H-AP, the residual SI after SIC can be approximated as $I_0 \sim CN(0, \alpha P_0)$, where $\alpha \ll 1$ [9]. Given the time allocation $\boldsymbol{\tau} = [\tau_1, \ldots, \tau_K]$, the achievable

---

[2] In practical scenarios, energy causality can also be considered, as studied in [5]. To focus on the FD operation at the UE, however, we do not consider the energy causality in this study. Specifically, we do not assume that U_i batteries are adequately charged at the start of each block. Nor do we assume that U_i's employ their respective harvested energy so that the energy charged in the battery at the end of each block reaches its initial state.

UL throughput of U_i during the ith slot is then given from (3) and (15) by

$$R_i(\boldsymbol{\tau}) = \tau_i \log_2\left(1+\frac{H_{0,i}P_i}{\Gamma(\sigma_0^2+\alpha P_0)}\right)$$

$$= \tau_i \log_2\left(1+\frac{\gamma_i(P_0)}{\tau_i}\right),\ i=1,\ldots,K, \tag{17}$$

where γ_i is given by

$$\gamma_i(P_0) = \frac{\rho_i H_{i,0} P_0}{\Gamma(\sigma_0^2+\alpha P_0)},\ i=1,\ldots,K. \tag{18}$$

Here, ρ_i, $i = 1, \ldots, K$, given in (16), and Γ represents the gap of the signal-to-interference-plus noise ratio (SINR) from the additive white Gaussian noise (AWGN) channel owing to the practical modulation and coding used.

2) Practical throughput achievable by partial knowledge of channels. In practice, it is difficult for the H-AP to obtain the knowledge of the channels between different UE, in other words, $H_{i,j}$, $i, j \in \{0, \ldots, K\}$, $i \neq j$, $i \neq 0$, $j \neq 0$. At a UE, furthermore, energy harvested from the transmissions of other UE is small enough to be negligible [1], [4]. Therefore, a practical throughput of a FD-WPCN-FD can be obtained by assuming that the H-AP only has the knowledge of $h_{0,i}$ and φ_i, $\forall i \in \{0, \ldots, K\}$, and by ignoring the energy harvested from the transmissions of other UE. In other words,

$$\sum_{j=1,\, j\neq i}^{K} \tau_j P_j H_{j,i} T = 0, \tag{19}$$

in (6). In this case, the amount of harvested energy at U_i in (10) is modified as

$$E_i^{\mathrm{h}} = \zeta_i\left(P_0 H_{0,i} + \tau_i P_i H_{i,i}\right)T. \tag{20}$$

By the same procedure from (7) through (12) with E_i^{h} replaced by (20), matrix $\mathbf{A}$ described in (13) is then modified as a diagonal matrix given by

$$A_{i,j} = \begin{cases} (1-\theta_i\varphi_i)/(1-\varphi_i) & ,\ \text{if } j=i, \\ 0 & ,\ \text{otherwise.} \end{cases} \tag{21}$$

Accordingly, ρ_i, $i = 1, \ldots, K$, in (15) is obtained by (16) and (21) as

$$\rho_i = \frac{(1-\varphi_i)}{(1-\theta_i\varphi_i)}\theta_i H_{0,i}. \tag{22}$$

The throughput of FD-WPCN-FD in this practical sense is then given by (17) and (18), where ρ_i in (18) is replaced by that in (22). As clearly shown in (17), (18), and (22), the throughput of the FD-WPCN-FD increases with θ_i. In other words, it increases with η_i or ζ_i since $\theta_i = \eta_i \zeta_i$.

2. Weighted Sum-Throughput Maximization

As shown in (17), the throughput of the FD-WPCN-FD can be maximized by optimizing the time allocated to each UE for a UL information transmission, denoted by $\boldsymbol{\tau} = [\tau_1, \ldots, \tau_K]$. Specifically, we maximize the weighted sum throughput in this network by solving the problem formulated as follows:

$$(\mathrm{P1}):\ \max_{t} \sum_{i=1}^{K} \omega_i R_i(t) \tag{23}$$

$$\text{s.t} \sum_{i=1}^{K} \tau_i \leq 1, \tag{24}$$

$$\tau_i > 0,\ i=1,\ldots,K. \tag{25}$$

It can be easily seen that problem (P1) is a convex optimization problem because $R_i(\boldsymbol{\tau})$ and (24) are concave and affine functions of $\boldsymbol{\tau}$, respectively. The optimal time allocation solution for (P1), denoted by $\boldsymbol{\tau}^*$, is then obtained as follows.

Proposition: The weighted sum throughput of the FD-WPCN-FD is maximized by the optimal time allocation solution for (P1), given by $\boldsymbol{\tau}^* = [\tau_1^*, \tau_2^*, \ldots, \tau_K^*]$ with

$$\tau_i^* = \frac{\gamma_i(P_0)}{z_i^*},\ i=1,\ldots,K, \tag{26}$$

where z_i^* denotes the solution of $f(z) = \lambda^* \ln 2/\omega_i$, with $f(z)$ defined as

$$f(z) \triangleq \ln(1+z) - \frac{z}{1+z}. \tag{27}$$

Proof: The proof is shown in Appendix A. ■

Figure 4 compares the achievable throughput region of the FD-WPCN-FD against those of the HD-WPCN and FD-WPCN-HD studied in [4], with $K = 2$, $P_0 = 20$ dB, $\sigma_0^2 = 0$ dB, and $\Gamma = 1$. Duplex modes of the H-AP and UEs in the HD-WPCN, FD-WPCN-HD, and FD-WPCN-FD are summarized in Table 1. It is assumed that $H_{0,1} = 0.50$, $H_{0,2} = 0.15$, and $H_{1,2} = H_{2,1} = 0.01$. For the FD-WPCN-HD, SIC at the H-AP is assumed to be perfect. For FD UEs in the FD-WPCN-FD, it is assumed that $\varphi_1 = \cdots = \varphi_K = 0.03$ with 15 dB of isolation between transmission and reception.

Considering the practical difficulty for the H-AP to obtain the knowledge of channels between different UEs, for all considered WPCNs, we assume that the H-AP has the knowledge of $H_{0,1}$ and $H_{0,2}$ only; the energy harvested from the transmissions of other UEs is thus ignored. In the

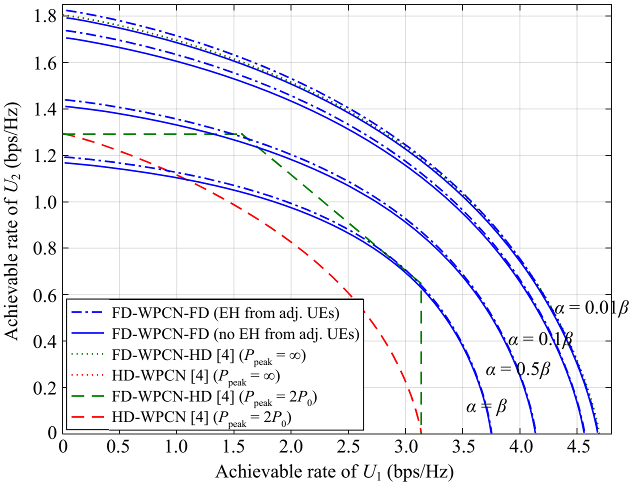

Fig. 4. Rate regions of WPCNs according to duplex modes.

Table 1. Comparison of duplex modes in various WPCNs.

	H-AP	UE
HD-WPCN	HD (TDD)	HD (TDD)
FD-WPCN-HD	FD	HD (TDD)
FD-WPCN-FD	FD	FD

case of FD-WPCN-FD, however, the ideal throughput obtained by (6) through (18) with the knowledge of $H_{1,2}$ and $H_{2,1}$ is also presented for the purpose of comparison.

It is shown in Fig. 4 that the throughput region of the FD-WPCN-FD is enlarged as α decreases (in other words, SIC performance improves). Moreover, the throughput of FD-WPCN-FD with consideration of energy harvested from the transmissions of other UE (blue dot–dash line in Fig. 4) is greater than the throughput of its counterpart (FD-WPCN-FD without consideration of energy harvested from transmissions of other UE; blue solid line). However, the increase is insignificant.

Figure 4 also compares the throughput region of FD-WPCN-FD obtained by (17) through (22) with those of HD-WPCN and FD-WPCN-HD when the energy harvested from the transmissions of other UE is not considered. It is observed from this figure that the throughput region of the FD-WPCN-FD when $\alpha = 0.5\beta$ with $\beta = \sigma_0^2/P_0$ is shown to be larger than those of HD-WPCN and FD-WPCN-HD with $P_{\text{peak}} = 2P_0$, where P_{peak} denotes the maximum peak transmit power at the H-AP in HD-WPCN and FD-WPCN-HD. In addition, when $\alpha = 0.01\beta$, the throughput region of the FD-WPCN-FD approaches those of HD-WPCN and FD-WPCN-HD with $P_{\text{peak}} = \infty$, which are theoretically maximum achievable throughput regions of HD-WPCN and FD-WPCN-HD.

Corollary: The sum throughput of the FD-WPCN-FD is maximized with a time allocation $\boldsymbol{\tau}^{\star} = [\tau_1^{\star}, \tau_2^{\star}, \ldots, \tau_k^{\star}]$, with

$$\tau_i^{\star} = \frac{\gamma_i(P_0)}{\sum_{j=1}^{K} \gamma_j(P_0)}, \quad i = 1, \ldots, K. \tag{28}$$

Proof: The proof is shown in Appendix B. ■

IV. Simulation Results

In this section, the sum throughputs of the HD-WPCN, FD-WPCN-HD, and FD-WPCN-FD are compared through simulations, with $K = 10$ and $\theta_i = 0.5$, $\forall i = 1, \ldots, K$. Duplex modes of the H-AP and UE in the aforementioned WPCNs follow those described in Table 1. We compare the practical throughput of these WPCNs by ignoring the energy harvested from the transmissions of other UE. For the FD-WPCN-FD, however, we also present the ideal throughput by considering the energy harvested from the transmissions of other UE for comparison. The bandwidth and noise spectral density are set as 1 MHz and −160 dBm/Hz, respectively. The UE is assumed to be uniformly distributed within two concentric circles, with diameters of 5 m and 10 m, respectively, where the H-AP is located at the center of these concentric circles. Assuming that the average signal power attenuation at a reference distance of 1 m is 30 dB, the channel power gain $H_{i,j}$ is modeled as $H_{i,j} = \upsilon_{i,j} 10^{-3} D_{i,j}^{-\delta}$, $\forall i, j = \{0, \ldots, K\}$, $i \neq j$, with $D_{i,j}$ denoting the distance between U_i and U_j in meters and the path loss exponent given by $\delta = 2$. In addition, we assume that the short-term fading, denoted by υ, is Rayleigh-distributed. That is, υ is an exponentially distributed random variable with a unit mean. For FD UE in FD-WPCN-FD, $\varphi_i = 0.03$, $\forall i = 1, \ldots, K$, assuming 15 dB of isolation between transmission and reception. Finally, we set $\Gamma = 9.8$ dB by assuming an uncoded quadrature amplitude modulation with the required bit-error rate given by 10^{-7} [10].

In Fig. 5, the maximum sum throughputs of the HD-WPCN, FD-WPCN-HD, and FD-WPCN-FD are compared with respect to the P_0 values in dBm. For both ideal and practical scenarios in FD-WPCN-FD, the throughput is obtained by assuming $\alpha = 0.01\beta$, with β defined in the previous section, whereas perfect SIC is assumed for the FD-WPCN-HD.

As shown in Fig. 5, in the FD-WPCN-FD, the difference between the sum throughput obtained with and without considering the energy harvested from transmissions of other UE is negligible. This verifies that

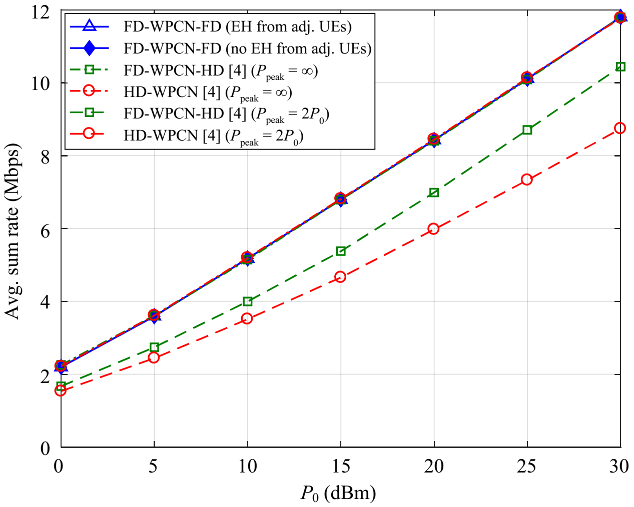

Fig. 5. Sum throughput vs. P_0.

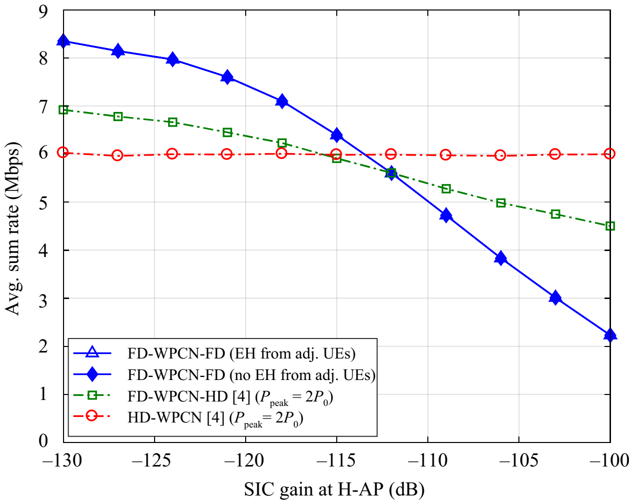

Fig. 6. Sum throughput vs. SIC gain at the H-AP.

the energy harvested from the transmissions of other UE has a minimal effect on the increase of throughput of FD-WPCN-FD. Furthermore, this implies that the throughput of the FD-WPCN-FD can be optimized, even with simpler approach presented in (17) through (22).

In addition, it is apparent in Fig. 5 that, even when the energy harvested from the transmissions of other UE is not considered, the average sum throughput of the FD-WPCN-FD is equivalent to those of the HD-WPCN and FD-WPCN-HD with $P_{\text{peak}} = \infty$. Note that the throughput of HD-WPCN and FD-WPCN-HD with $P_{\text{peak}} = \infty$ is an ideal throughput that is only theoretically achievable; it is not achievable in practice. Given that the power of residual SI after SIC is sufficiently close to the level of background noise, the FD-WPCN-FD can achieve the throughput equivalent to the theoretically maximum ones of HD-WPCN and FD-WPCN-HD, even with practical settings and a simple resource allocation algorithm.

Compared to the FD-WPCN-HD with $P_{\text{peak}} = 2P_0$, finally, the FD-WPCN-FD achieves a sum throughput gain of 4 dB with respect to P_0. Furthermore, the sum throughput of the FD-WPCN-FD is shown to increase more quickly with the increase in P_0 than that of the HD-WPCN with $P_{\text{peak}} = 2P_0$.

Figure 6 compares the maximum sum throughput of the aforementioned WPCNs for different values of SIC gain, where the SIC gain is defined as $1/\alpha$. The sum throughput of the FD-WPCN-FD is shown to be greater than those of the HD-WPCN and FD-WPCN-HD when the SIC gain at the H-AP is greater than 114 dB. In other words, the power of the residual SI after SIC is $4\sigma_0^2$. Note that current SIC technologies (for example, [2] and [3]) reduce the power of the residual SI sufficiently close to σ_0^2 after SIC. Even with current SIC technologies at the H-AP, therefore, the use of the FD UE shown in Fig. 2 efficiently improves the throughput of the WPCN. When α is 120 dB, in other words, the aggregated power of residual SI and background noise is $4\sigma_0^2$, FD-WPCN-FD achieves 18% and 25% of throughput gain compared to FD-WPCN-HD and HD-WPCN, respectively.

Finally, Fig. 7 shows the throughput of the FD-WPCN-FD with respect to the circulator leakage φ_i. When $\varphi_i = 0$ dB, the throughput of the FD-WPCN-FD is zero because the whole energy at PA output leaks into the energy harvester and thus information is not transmitted. When $\varphi_i \neq 0$, a trade-off associated with the value of φ_i is observed. The throughput of FD-WPCN FD decreases with increasing φ_i when $\varphi_i \leq 3$ dB because the increase of the harvested energy owing to greater SI is dominant

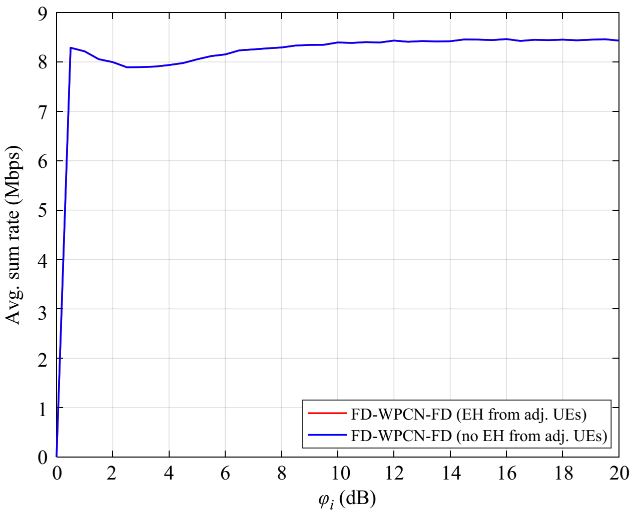

Fig. 7. Sum throughput vs. φ_i at the UE.

when φ_i is small. When $\varphi_i \geq 3$ dB, on the other hand, the throughput increases with φ_i because more energy utilization for WIT with smaller φ_i is more beneficial when φ_i is adequately large, although the amount of the harvested energy decreases. However, the effect of the trade-off associated with φ_i on the throughput of FD-WPCN-FD is observed to be insignificant as long as $\varphi_i \neq 0$. Finally, the throughput of FD-WPCN-FD converges when $\varphi_i \geq 14$ dB.

V. Conclusion

This paper described a WPCN, where both the H-AP and UE operate in FD mode. Owing to the FD capability, UE can receive energy and transmit information simultaneously in the DL and UL, respectively. We first proposed an FD transceiver structure for UE that enables simultaneous energy reception and information transmission. We then provided an energy usage model in the proposed UE transceiver. Furthermore, an optimal time allocation solution to maximize the weighted sum throughput of the WPCN with the FD H-AP and FD UE was obtained for both cases in which the energy harvested from the transmissions of other UE respectively was and was not considered. It was shown that the use of the proposed FD UE, as well as an FD H-AP with practical SIC capability, significantly improved the WPCN throughput. In addition, the use of FD H-AP and FD UE was shown to enable WPCN to achieve the throughput equivalent to the theoretically maximum ones of conventional HD-WPCN and FD-WPCN-HD, even with practical settings and a simple resource allocation algorithm.

Acknowledgements

This work was partly supported by the Institute for Information and Communications Technology Promotion (IITP) grant (No. 2014-0-00282, Development of 5G Mobile Communication Technologies for Hyper-Connected Smart Services) and Cross-Ministry Giga Korea Project grant (No. GK17P0500, Development of Ultra Low-Latency Radio Access Technologies for 5G URLLC Service), both funded by the Korean government (MSIT).

Appendix A. Proof of Proposition

From (23) through (25), we have the Lagrangian of (P1) as

$$\mathcal{L}(\boldsymbol{\tau}, \lambda) = \sum_{i=1}^{K} \omega_i R_i(t) - \lambda\left(\sum_{i=1}^{K} \tau_i - 1\right), \qquad (29)$$

with $\lambda \geq 0$ representing the Lagrange multiplier associated with (24). We thus have the dual function of (P1) as:

$$\mathcal{G}(v) = \min_{t \in \mathcal{D}} \mathcal{L}(\boldsymbol{\tau}, \lambda), \qquad (30)$$

with $\mathcal{D}$ denoting the feasible set of $\boldsymbol{\tau}$ specified by (24) and (25). Note that Slater's condition holds for (P1) because we can find a $\boldsymbol{\tau} \in \mathcal{D}$, $\tau_i > 0$, $i = 1, \ldots, K$, through which

$$\sum_{i=1}^{K} \tau_i < 1.$$

Therefore, (P1) is shown to be a convex optimization problem for which the strong duality holds, and the globally optimal solution for (P1) thus satisfies the Karush–Kuhn–Tucker conditions [11] given by

$$\sum_{i=1}^{K} \tau_i^* \leq 1, \qquad (31)$$

$$\lambda^*\left(\sum_{i=1}^{K} \tau_i^* - 1\right) = 0, \qquad (32)$$

$$\frac{\partial}{\partial \tau_i} \sum_{i=1}^{K} R_i(\boldsymbol{\tau}^*) - \lambda^* = 0, \;\; i = 0, \ldots, K, \qquad (33)$$

with τ_i*'s and λ* denoting the optimal primal and dual solutions of (P1), respectively. With no loss of generality, we can assume $\lambda^* > 0$ from (32) because

$$\sum_{i=1}^{K} \tau_i^* = 1$$

must hold for (P1). From (33), it then follows that

$$\ln\left(1 + z_i^*\right) - \frac{z_i^*}{1 + z_i^*} = \frac{\lambda^* \ln 2}{\omega_i}, \; i = 1, \ldots, K, \qquad (34)$$

where $z_i^* = \gamma_i(P_0)/\tau_i^*$. Note that $f(z)$ in (27) is a monotonically increasing function of z with $f(0) = 0$ and $f(\infty) = \infty$. Therefore, $\boldsymbol{\tau}^*$ is uniquely obtained for the given values of $\gamma_i(P_0)$. The proof of proposition is completed.

Appendix B. Proof of Corollary

The sum throughput of this network is maximized by solving (P1) with $\omega_1 = \omega_2 = \cdots = \omega_K = 1/K$. For the inequality in (34) to hold in this case, we should have

$$\frac{\gamma_1(P_0)}{\tau_1^\bigstar} = \frac{\gamma_2(P_0)}{\tau_2^\bigstar} = \cdots \frac{\gamma_K(P_0)}{\tau_K^\bigstar}. \qquad (35)$$

From (32) and (35), it follows that

$$\sum_{i=1}^{K} \tau_i^{\star} = \frac{\tau_i^{\star}}{\gamma_i} \sum_{j=1}^{K} \gamma_j = 1, \tag{36}$$

and from (36), the optimal time allocation solution in (28) is obtained. The corollary is now proved.

References

[1] H. Ju and R. Zhang, "Throughput Maximization in Wireless Powered Communication Networks," *IEEE Trans. Wireless Commun.*, vol. 13, no. 1, Jan. 2014, pp. 418–428.

[2] D. Bharadia, E. McMilin, and S. Katti, "Full Duplex Radios," in *Proc. ACM SIGCOMM*, Hong Kong, China, Aug. 2013, pp. 375–386.

[3] M. Chung et al., "Prototyping Real-Time Full Duplex Raios," *IEEE Commun. Mag.*, vol. 53, no. 9, Sept. 2015, pp. 56–63.

[4] H. Ju and R. Zhang, "Optimal Resource Allocation in Full-Duplex Wireless Powered Communication Network," *IEEE Trans. Commun.*, vol. 62, no. 10, Oct. 2014, pp. 3528–3540.

[5] X. Kang, C.K. Ho, and S. Sun, "Full-Duplex Wireless Powered Communication Network with Energy Causality," *IEEE Trans. Wireless Commun.*, vol. 14, no. 10, Oct. 2015, pp. 5539–5551.

[6] H. Kim et al., "Joint Subcarrier and Power Allocation Methods in Full Duplex Wireles Powered Communication Networks for OFDM Systems," *IEEE Trans. Wireless Commun.*, vol. 15, no. 7, July 2016, pp. 4745–4753.

[7] Y. Zeng and R. Zhang, "Full-Duplex Wireless-Powered Relay With Self-Interference Recycling," *IEEE Trans. Wireless Commun.*, vol. 15, no. 7, July 2016, pp. 4745–4753.

[8] H. Ju, K. Chang, and M.-S. Lee, "In-band Full-Duplex Wireless Powered Communication Networks," in *Proc. IEEE Int. Conf. Adv. Commun. Tech. (ICACT)*, Pyeongchang, Rep. of Korea, July 2015, pp. 23–27.

[9] B.P. Day et al., "Full-Duplex Bidirectional MIMO: Achievable Rates Under Limited Dynamic Range," *IEEE Trans. Signal Process*, vol. 60, no. 7, July 2012, pp. 3702–3716.

[10] A. Goldsmith, *Wireless Communications*, New York, USA: Cambridge University Press, 2005.

[11] S. Boyd and L. Vandenberghe, *Convex Optimization*, New York, USA: Cambridge University Press, 2004.

Hyungsik Ju received BS and PhD degrees in Electrical Engineering from Yonsei University, Seoul, Rep. of Korea, in 2005 and 2011, respectively. From 2011 to 2012, he worked as a researcher at Yonsei University. From 2012 to 2014, he was with the Department of Electrical and Computer Engineering of the National University of Singapore, as a research fellow. Since 2014, he has been with ETRI, Daejeon, Rep. of Korea, as a senior researcher. His current research interests include full-duplex wireless communication, wireless information and power transfer, wireless powered networks, relay-based multi-hop communication, and full-duplex relay systems.

Yuro Lee received BS and MS degrees in electrical engineering from Seoul City University, Rep. of Korea in 1997 and 1999, respectively. Since 2001, he has been with ETRI, Daejeon, Rep. of Korea, where he is currently a principal research engineer. His current research interests are broadband wireless transmission technologies and 5G mobile communications.

Tae-Joong Kim received BS, MS, and PhD degrees from Yonsei University, Seoul, Rep. of Korea, in 1991, 1993, and 1998, respectively. From 1998 to 2000, he was a senior researcher of ETRI, Daejeon, Rep. of Korea. He joined Eonex, Ltd., Rep. of Korea in 2001, where he first worked on chipset system design and later software protocol stack and field testing until 2006. He returned to ETRI in 2006 and developed 4G-LTE and 5G mobile communication systems. He is currently the managing director of the Mobile Transmission Research Department at ETRI and manages 5G projects sponsored by the government.